

Poiseuille flow of liquid methane in nanoscopic graphite channels by molecular dynamics simulation

M. Horsch¹, J. Vrabec^{*,1}, M. Bernreuther², and H. Hasse³

September 15, 2021

¹University of Paderborn, Thermodynamics and Energy Technology Laboratory (ThEt), Warburger Str. 100, 33098 Paderborn, Germany

²High Performance Computing Center Stuttgart (HLRS), Department Parallel Computing – Training & Application Services, Nobelstr. 19, 70569 Stuttgart, Germany

³University of Kaiserslautern, Laboratory of Engineering Thermodynamics (LTD), Erwin-Schrödinger-Str. 44, 67663 Kaiserslautern, Germany

1 Introduction

On the nanometer length scale, continuum approaches like the Navier-Stokes equation break down [1]. Therefore, the study of nanoscopic transport processes requires a molecular point of view and preferably the application of molecular dynamics (MD) simulation. In the past, MD could be applied to small systems with a few thousand particles only, due to the low capacity of computing equipment. Consequently, a large gap between MD simulation results on the one hand and experimental results as well as calculations based on continuum methods was present.

The constant increase in available computational power is eliminating this barrier, and the characteristic length of the systems accessible to MD simulation approaches micrometers. However, this can only be realized by laying an emphasis on the simplicity of the molecular models and an efficient implementation, suitable for massively parallel processing.

Due to their anisotropy, nanostructures containing graphite and carbon nanotubes are of particular interest. The present work deals with the flow behavior of

*Author to whom correspondence should be addressed: jadran.vrabec@upb.de.

liquid methane, modeled by the truncated and shifted Lennard-Jones (LJ/TS) potential [2], confined between graphite walls. It covers nanoscopic Poiseuille flow up to a channel width of $0.135 \mu\text{m}$.

2 Simulation method and scalability

With the potential parameters $\sigma_f = 3.7241 \text{ \AA}$ and $\varepsilon_f/k_B = 175.06 \text{ K}$, the LJ/TS potential is known to be an accurate model for methane that covers the thermodynamic properties of the fluid quantitatively [3]. Following a widespread approach introduced by Battezzati *et al.* [4], the interaction between methane molecules and the carbon atoms begin part of a graphite surface can also be described by a Lennard-Jones potential. The present study applies the LJ/TS potential to the interaction between methane molecules and carbon atoms as well, using the potential parameters proposed for graphite by Wang *et al.* [5], $\sigma_w = 3.3264 \text{ \AA}$ and $\varepsilon_w = 0.00188 \text{ eV}$. The unlike interaction parameters σ_{fw} and ε_{fw} , acting between methane and carbon, were determined according to the Lorentz-Berthelot mixing rule.

Carbon and silicon structures as well as ceramics can well be represented by the Tersoff potential [6, 7], which permits to predict many properties of these systems with a good accuracy [8]. For graphite, however, the bond length corresponding to the Tersoff potential (1.461 \AA), cf. Kelires [9], deviates considerably from the actual value of 1.421 \AA [10]. Therefore, the relevant Tersoff potential parameters for the wall model were rescaled in the present study.

The present version of the employed **LS1/Mardyn** MD simulator uses a spatial domain decomposition with equally sized cuboid subdomains and a cartesian topology based on linked cells [11]. Often the best solution is an ‘isotropic’ decomposition that minimizes the surface to volume ratio of the spatial subdomains. For the simulation of homogeneous systems, this approach is quite efficient [12]. That is underlined by the weak and strong scaling behavior of **LS1/Mardyn** for typical configurations, shown in Fig. 1 (left), in cases where supercritical methane (‘fluid’) at $\rho = 10 \text{ mol/l}$ and solid graphite (‘wall’) were considered with a system size of up to 4,800,000 interaction sites, representing the same number of carbon atoms and methane molecules here. Graphite simulations, where only the carbon wall atoms are regarded, scale particularly well, due to a favorable relation of the delay produced by communication between processes to the concurrent parts, i.e., the actual intermolecular interaction computation, which is much more expensive for the Tersoff potential than the LJ/TS potential.

The simulation of the regarded combined systems, containing both fluid and solid interaction sites, is better handled by a channel geometry based decomposi-

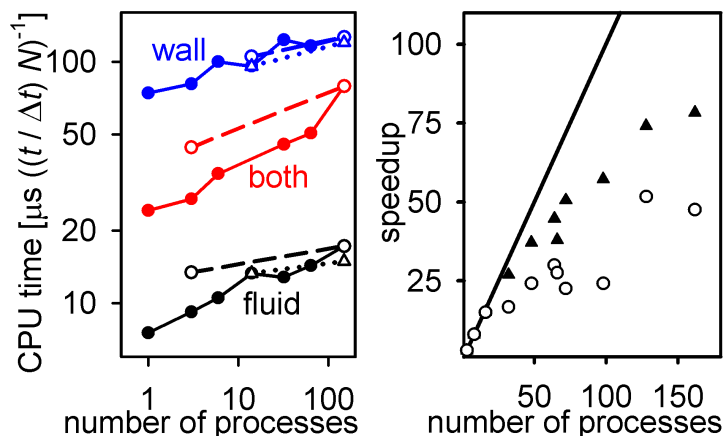


Figure 1: Left: total CPU time, i.e., execution time multiplied with the number of parallel processes, per time step and interaction site for weak scaling with 3,000 (dashed lines / circles) and 32,000 (dotted lines / triangles) interaction sites per process as well as strong scaling with 450,000 interaction sites (solid lines / bullets), using isotropic spatial domain decomposition. Right: speedup, i.e., sequential execution time divided by parallel execution time, for a system of liquid methane between graphite walls with 650,000 interaction sites, where isotropic (circles) and channel geometry based (triangles) spatial domain decomposition was used; the solid line represents optimal speedup.

tion scheme, where an approximately equal portion of the wall and a part of the fluid is assigned to each process, cf. Fig. 1 (right). In the general case, where spatial non-uniformities do not match any cartesian grid, a flexible topology has to be used. An approach based on k -dimensional trees [13, 14], implemented in a version of **LS1/Mardyn**, showed clearly improved results with respect to the scaling of inhomogeneous systems.

3 MD flow simulation of liquid methane

The **LS1/Mardyn** MD program was used to conduct a series of Poiseuille flow simulations with liquid methane in the canonical ensemble. The flow was induced by an external gravitation-like acceleration acting on all fluid molecules. Analogously, Couette flow was simulated by accelerating only the wall atoms. A PI controller

$$\tau^2 \dot{a}_z(t) = \bar{v}_z - 2v_z(t) + v_z(t - \tau'), \quad (1)$$

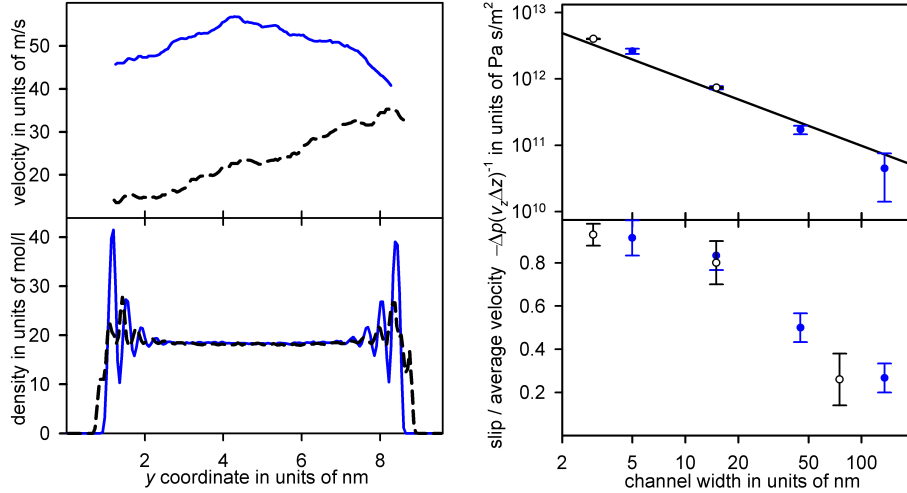


Figure 2: Left: velocity profile (top) and density profile (bottom) for Poiseuille (solid lines) and Couette (dotted lines) flow of liquid methane at $T = 166.3$ K with a channel width of $h = 8$ nm and a characteristic flow velocity of $\bar{v}_z = 50$ m/s. Right: pressure drop $-\Delta p$ in terms of \bar{v}_z and the channel length Δz (top) as well as slip velocity in terms of \bar{v}_z (bottom), for Poiseuille flow of saturated liquid methane at a temperature of $T = 166.3$ K and average velocities \bar{v}_z of 10 m/s (circles) and 30 m/s (bullets), in dependence of the channel width; solid line: Darcy's law.

was applied to the acceleration a_z for a flow in z direction with a characteristic velocity of \bar{v}_z , where $v_z(t)$ is the velocity at a given time, τ was on the order of 1 – 100 ps and τ' on the order of 0.1 – 10 ps. Velocity and density profiles, cf. Fig. 2 (left), and the average acceleration were extracted from the simulations.

It is known for Poiseuille flow with channel widths h below 2 nm that the slip velocity can reach values above $0.99 \bar{v}_z$, a regime which was studied by Sokhan *et al.* [15] for methane in carbon nanotubes. Velocity profiles with a strong influence of boundary slip were also found in some of the present simulations, cf. Fig. 2 (left). For channel widths between $h = 20$ and 50 nm, the boundary slip undergoes a transition, as shown in Fig. 2 (right). For h down to molecular length scales, the pressure drop $-\Delta p$ is approximately proportional to the average velocity \bar{v}_z and inversely proportional to cross-sectional area of the channel, corresponding to cf. Fig. 2 (right), in agreement with Darcy's law.

4 Conclusion

The scalability of the **LS1/Mardyn** program, optimized for massively parallel MD simulations of simple fluids interacting with carbon nanostructures, was assessed and found to be satisfactory. MD simulations of methane confined between graphite walls with up to 4,800,000 interaction sites, i.e., carbon atoms and methane molecules, were conducted to demonstrate the viability of the program.

The channel width was varied to include both the boundary-dominated regime and the transition to the continuum regime. This proves that MD can be used today to cover the entire range of characteristic lengths for which continuum methods fail. The simulation results show that the transition between both regimes occurs in a relatively narrow region, between $h = 20$ and 50 nm in the present case. For a flow velocity up to 30 m/s, it was confirmed for methane in graphite channels that Darcy's law applies on both sides of this transition.

Acknowledgements

The authors would like to thank M. Buchholz for contributing to **LS1/Mardyn**, F. Gähler and M. Heitzig for their proposals concerning the wall model as well as J. Harting and M. Hecht for discussions. The scaling of **LS1/Mardyn** was measured on the *cacau* supercomputer at HLRS. The other simulations were performed on the HP XC6000 supercomputer at the Steinbuch Centre for Computing, Karlsruhe, under the grant LAMO.

References

- [1] G. Karniadakis, A. Beskok, and N. Aluru. *Microflows and Nanoflows: Fundamentals and Simulation*. Springer, New York, 2005.
- [2] M. P. Allen and D. J. Tildesley. *Computer Simulation of Liquids*. Clarendon, Oxford, 1987.
- [3] J. Vrabec, G. K. Kedia, G. Fuchs, and H. Hasse. Comprehensive study on vapour-liquid coexistence of the truncated and shifted Lennard-Jones fluid including planar and spherical interface properties. *Mol. Phys.*, 104:1509–1527, 2006.
- [4] L. Battezzati, C. Pisani, and F. Ricca. Equilibrium conformation and surface motion of hydrocarbon molecules physisorbed on graphite. *J. Chem. Soc. Faraday Transact. 2*, 71:1629–1639, 1975.

- [5] Y.-C. Wang, K. Scheerschmidt, and U. Gösele. Theoretical investigations of bond properties in graphite and graphitic silicon. *Phys. Rev. B*, 61:12864–12869, 2000.
- [6] J. Tersoff. Empiric interatomic potential for carbon, with applications to amorphous carbon. *Phys. Rev. Lett.*, 61:2879–2882, 1988.
- [7] J. Tersoff. Modeling solid-state chemistry: Interatomic potentials for multi-component systems. *Phys. Rev. B*, 39:5566–5568, 1989.
- [8] N. Resta. *Molecular dynamics simulations of precursor-derived Si–C–N ceramics*. PhD thesis, Universität Stuttgart, Institute for Theoretical and Applied Physics, 2005.
- [9] P. C. Kelires. Structural properties and energetics of amorphous forms of carbon. *Phys. Rev. B*, 47:1829–1839, 1993.
- [10] A. F. Holleman and N. Wiberg. *Inorganic Chemistry*. Academic Press, San Diego, 2001.
- [11] M. Bernreuther and J. Vrabec. Molecular simulation of fluids with short range potentials. In M. Resch et al., editors, *High Performance Computing on Vector Systems*, pages 187–195, Heidelberg, 2006. Springer.
- [12] J. J. Morales and S. Toxværd. The cell-neighbour table method in molecular dynamics simulations. *Comp. Phys. Comm.*, 71:71–76, 1992.
- [13] J. L. Bentley. Multidimensional binary search trees used for associative searching. *CACM*, 18:509–517, 1975.
- [14] J. L. Bentley. Multidimensional Divide and Conquer. *CACM*, 23:214–229, 1980.
- [15] V. P. Sokhan, D. Nicholson, and N. Quirke. Fluid flow in nanopores: Accurate boundary conditions for carbon nanotubes. *J. Chem. Phys.*, 117:8531–8539, 2002.